

Multiple-scattering calculations of electron-energy-loss near-edge structures of existing and predicted phases in the ternary system B-C-N

M. Wibbelt and H. Kohl

Physikalisches Institut der Westfälischen Wilhelms-Universität, Wilhelm-Klemm Straße 10, D-48149 Münster, Germany

Ph. Kohler-Redlich

Max-Planck-Institut für Metallforschung, Seestraße 92, D-70174 Stuttgart, Germany

(Received 11 August 1998)

The electron-energy-loss near-edge structures (ELNES) of the B *K*, C *K*, and N *K* ionization edges of different phases in the boron-carbon-nitrogen (B-C-N) system are calculated using a multiple scattering (MS) approach. A comparison of calculated and experimental spectra for cubic diamond, graphite, cubic (*c*-BN) and hexagonal (*h*-BN) boron nitride is made to judge the reliability of the MS approach. The calculations are found to reproduce the main features of the experimental ELNES. However, in the quantitative comparison the peak positions deviate up to 3 eV. The multiple-scattering approach is applied to predict the ELNES of three hypothetical phases, namely, BC₂N, BC₃, and β -C₃N₄, for which no accepted experimental reference spectra exist. Our results demonstrate the usefulness of MS calculations to predict the ELNES of novel phases as a tool for future experimental characterization. [S0163-1829(99)02418-2]

I. INTRODUCTION

The development of new boron-carbon-nitrogen (B-C-N) materials is of considerable interest in materials science. The structural similarity of graphite and hexagonal boron nitride (*h*-BN) has motivated the synthesis of new alloys of these two phases. Graphite is a semimetal and forms a large variety of intercalation compounds, whereas *h*-BN is an insulator and a very limited host material. Due to their isogeometric and isoelectronic structures, graphite and *h*-BN are expected to form new hybrid B-C-N materials, which should have semiconducting properties and a tunable band gap depending on composition. The existence of phases as BC₂N (Ref. 1) or BC₃ (Refs. 2 and 3) have been predicted theoretically.

The first hybrid of composition BC₂N has been synthesized by Kouvetakis *et al.*⁴ using CVD with BCl₃ and CH₃CN as starting materials. Hexagonal BC₂N can be either metallic or semiconducting depending on whether the structure possesses inversion symmetry or not.¹ The first synthesis of a BC₃ phase derived from interaction of BCl₃ and benzene (C₆H₆) at 800 °C by substitution of boron atoms into the hexagonal network of the graphite structure was reported by Kouvetakis *et al.*⁵ Owing to the substitution of every fourth carbon atom by boron BC₃ is lighter and has improved electrical conductivity compared to graphite. Since the discovery of carbon nanotubes in 1991,⁶ B-C-N nanotubes with BC₂N (Refs. 7–9) and BC₃ (Refs. 9 and 10) structures have been studied extensively both experimentally and theoretically. As part of the search for new ultrahard materials the carbon nitride phase, β -C₃N₄, has received remarkable attention. This compound was predicted by Liu and Cohen¹¹ and is based on the known β -Si₃N₄ structure with carbon substituted for silicon. So far, considerable efforts have been directed towards the synthesis of β -C₃N₄.^{12–15} It is predicted that β -C₃N₄ is metastable and possesses a hardness comparable to or higher than diamond.^{11,16} The possible syntheses

routes, the structures, the basic properties, and the potential applications of B-C-N, B-C, and C-N materials have recently been summarized by Kawaguchi.¹⁷

The syntheses of macroscopic quantities of these phases, however, has been realized to be a considerably difficult task most likely due to their metastability. The products of syntheses are generally small particles or multiphase samples, for which phase identification is not straightforward. Electron-energy-loss spectroscopy (EELS) in a transmission electron microscope with high spatial resolution has been an important tool to investigate such products with respect to their structure and chemistry.¹⁸ For light elements like boron, carbon, and nitrogen EELS is an especially suitable technique to obtain both chemical composition and structural information on local scale.¹⁹ It is well known that the characteristic fine structure in the first few tens of eV beyond the onset of the core loss ionization edges (ELNES) provides so-called coordination fingerprints, which can be used to identify phases in complex systems²⁰ or even to study phase transformations in nanoscale particles.²¹ The usual procedure is the collection of experimental spectra from reference samples which serve as database for future phase identification; for the B-C-N system see, for example, the recent review of Schmid²² or the detailed discussion of the C *K* ELNES in graphite by Batson.²³ In the case of hypothetical, theoretically predicted phases in the B-C-N system no such reference spectra exist. Therefore a theoretical approach to simulate the ELNES of such phases is desirable. In the present work we calculate the ELNES of the *K* (1*s*) ionization edges of BC₂N, BC₃, and β -C₃N₄ using an updated version of the ICXANES code provided by Durham, Pendry, and Hodges,²⁴ and Vvedensky, Saldin, and Pendry.²⁵

Multiple scattering methods have been used by other groups to investigate the ELNES of materials like diamond,^{26–29} graphite,^{27,30} cubic³¹ and hexagonal boron nitride.^{31,32}

II. CALCULATIONAL DETAILS

The calculation of ELNES using a multiple-scattering approach is based on the interference between the outgoing electron wave generated by the ejection of an inner-shell electron and the electron wave elastically backscattered from the surrounding atoms.^{33,34} The origin of this approach is in the study of x-ray-absorption near-edge structures (XANES), but for small collection angles where the momentum transfer is small and dipole transitions dominate, the interpretation of ELNES is the same.¹⁸ The formalism of the MS theory is equivalent to the Korringa-Kohn-Rostocker (KKR) band theory.³⁵ In the simple one-electron picture the observed near-edge structures reflect the symmetry-projected density of unoccupied states above the Fermi level.³⁶ But according to a study of rutile and anatase by Brydson *et al.*,³⁷ we also have to consider many-electron effects for the explanation of the resulting ELNES.

The input data for the ICXANES code²⁵ are (i) the cluster coordinates of the atoms subdivided into shells surrounding the absorbing atom, (ii) the matrix elements for the transition of an electron from the $1s$ state of the central atom to the conduction band, and (iii) the phase shifts for incident spherical waves with angular momenta up to $l_{max}=3$ (i.e., s to f symmetry), describing the scattering properties of each type of atom.

Phase shifts as well as matrix elements were calculated assuming a muffin-tin shape for the crystal potential formed from atomic potentials according to Mattheiss prescription^{38,39} for the superposition of neutral atomic charge densities derived from atomic self-consistent field (SCF) X_α wave functions.⁴⁰ The so-called ($Z+1$) approximation for the absorbing atom⁴¹ is used to consider the core-hole effects which can be considerable for low Z element K edges.⁴² The local exchange parameter α (Ref. 43) was taken to be 0.8 for all calculations and the muffin-tin radii were chosen to be half of the nearest-neighbor distances. Besides that, the inelastic attenuation parameter SE , which is the imaginary part added to the energy of the excited electron, can be used to include the experimental broadening.^{30,44} It is a common approach to choose the value of SE equal to the instrumental energy resolution, as defined by the full width at half maximum (FWHM) of the zero loss peak. However, the chromatic aberrations of the spectrometer can lead to a further reduction of the effective energy resolution for the core edges depending on their energy loss. The convolution of the calculated spectra with appropriately chosen Lorentzian functions can be used to handle this effect and to aim for a higher similarity of the calculated to the experimental data (see, e.g., Ref. 45). We have decided against a fitting of the energy broadening and present all calculated spectra in this paper with $SE=0.5$ eV. The main discrepancies observed in this investigation are shifts of the peak energies, which do not depend on broadening effects.

The calculations were performed in real space by dividing the cluster into concentric shells of atoms surrounding the central atom. The multiple scattering of the whole cluster is determined with intrashell and intershell scattering. The first ten shells were considered corresponding to a cluster radius of approximately 10 a.u. (100–150 atoms, 1 a.u. = 0.529 Å).

The crystal structures for cubic diamond, graphite, c -BN and h -BN were taken from Ref. 46; the models for the other phases are described in Sec. IV B. For the layered compounds, graphite, and h -BN, the spectra for the two inequivalent atom positions have been calculated separately and weighted to equal amounts in the spectra presented.

In the calculation of near-edge structures the crystal orientation with respect to the incident electron beam has to be considered. It is known for layered structures like graphite and h -BN to show a large degree of anisotropy as revealed by earlier XANES and ELNES investigations.^{47–49} In our calculations parameter settings were used (no polarization, Ref. 25) which leads to an averaging over all possible incident-beam directions. This situation corresponds to the signal expected in x-ray absorption or EEL spectroscopy from polycrystalline samples. Anisotropy or polarization effects in general do change the intensity of peaks but do not shift their positions. Only for overlapping peaks, which are too close to be resolved, the dependence of relative peak intensities on the incident beam-direction may result in an apparent energy shift of the combined peak. This energy shift can amount up to the energy difference of the two peaks and is hence in the order of or smaller than the instrumental energy resolution.

III. EXPERIMENTAL DETAILS

The experimental ELNES (the two spectra of c -BN were provided by J. Loeffler⁵⁰) were recorded with a Gatan 666 parallel electron energy-loss spectrometer attached to a VG HB501UX dedicated scanning transmission electron microscope (STEM) operating at 100 kV accelerating voltage. Effective collection angles of 6.5 and 13 mrad have been used. In general this is small enough⁵² to be in the regime of small momentum transfer and for thin samples the observed transitions should obey the dipole selection rules, i.e., for K edges the final state is predominantly p -like. For the different measurements the energy resolution of the system was in the range of 0.6–1.1 eV (FWHM of the zero loss peak). All spectra were corrected for dark current and detector gain variations. A background of the form AE^{-r} with the adjustable parameters A and r has been subtracted from each spectrum. The effects of inelastic scattering were removed by applying a Fourier-Ratio deconvolution.¹⁸ Zero loss peak deconvolution was applied to correct for the instrumental broadening function.¹⁸ All data processing was performed with the Gatan EL/P 3.0 program. Details about the reference samples used to obtain the experimental spectra are given in Ref. 51.

IV. RESULTS AND DISCUSSION

A. Existing phases

Figures 1–3 compile the calculated K edge ELNES of cubic diamond, graphite, cubic (c -BN), and hexagonal (h -BN) boron nitride in comparison to the experimental reference spectra. The spectra are plotted versus electron-energy loss. The absolute energy values for the K edges, as measured at half height of the edge onset in the experimental spectra, are listed in Table I. The baseline is arbitrarily chosen for clarity of presentation. The total intensities under the

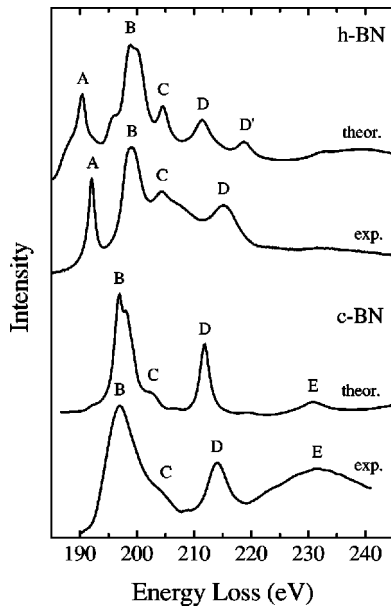


FIG. 1. Experimental (exp.) and theoretical (theor.) B K ELNES of *c*-BN and *h*-BN. The positions of the marked peaks are given in Table II.

edges are normalized to area. Owing to the arbitrariness of the muffin-tin potential zero, all calculated spectra are shifted in a way that the position of the main peak coincides with the corresponding experimental one. The positions of the most prominent peaks (labeled A to E) in Figs. 1–3 relative to the main σ^* peak B are collected in Table II.

In agreement with previous measurements^{22,30,53} the displayed experimental spectra point out the differences in the bonding characteristics of the hexagonal and cubic phases. The *K* ELNES of graphite and *h*-BN (Figs. 1–3) show two separate peaks (A, B) at the edge onset in contrast to the cubic phases diamond and *c*-BN, which show only one peak (B). The additional feature A in the spectra of the hexagonal

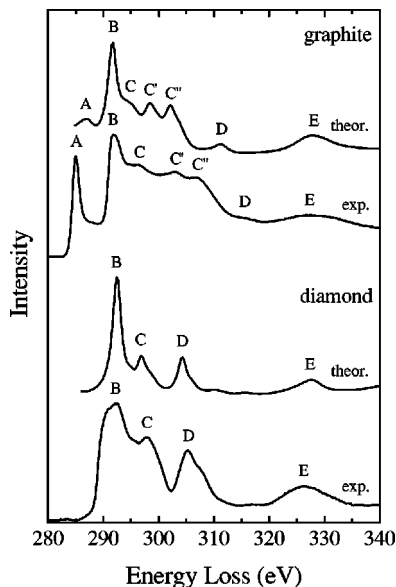


FIG. 2. Experimental (exp.) and theoretical (theor.) C K ELNES of cubic diamond and graphite. The positions of the marked peaks are given in Table II.

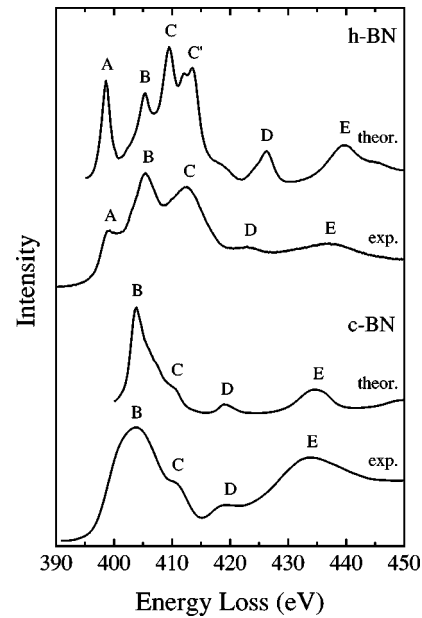


FIG. 3. Experimental (exp.) and theoretical (theor.) N K ELNES of *c*-BN and *h*-BN. The positions of the marked peaks are given in Table II.

phases present in the B, C, and N *K* edges corresponds to transitions of the $1s$ electrons to the empty π^* antibonding orbitals. This characteristic peak is widely used to identify sp^2 -hybridized materials. The series of peak B to D is related to $1s \rightarrow \sigma^*$ transitions.⁴⁷ The broad feature E is part of the extended energy-loss fine structure (EXELFS) due to backscattering from nearest neighbors.¹⁸ The π^* structures are absent in the ELNES of the cubic phases. The spectrum is dominated by peak B. All cubic phases show consistently the higher energy features D and E, the latter being again an EXELFS oscillation. Peak C is clearly visible for diamond and appears as a shoulder for the B *K* and N *K* edges in *c*-BN.

The characteristic distinction of the ELNES between the cubic and the hexagonal phases for all *K* edges is clearly reproduced by the calculations. Specifically, the π^* feature is only visible for the *K* edges of the hexagonal phases. Also the existence of the features B to E in the spectra shows reasonable correspondence between theory and experiment. The relative intensities of the peaks with respect to each other follow the correct trends with some exceptions. This is more satisfactory for the cubic than for the hexagonal phases. However, the relative peak positions compared in Table II reveal a misalignment of corresponding features by up to 3

TABLE I. Absolute electron-energy losses (± 0.1 eV) of the *K* edges in the experimental spectra labeled in Figs. 1–3.

Phase	Ionization edge (eV)		
	B <i>K</i>	C <i>K</i>	N <i>K</i>
Diamond	-	287.9	-
Graphite	-	284.3	-
<i>c</i> -BN	194.5	-	397.4
<i>h</i> -BN	191.4	-	398.9

TABLE II. Positions of peaks A to E in the spectra in Figs. 1–3. All positions are given relative to the main σ^* peak B. The estimated error is 0.2 eV.

Phase	Edge		Peak position relative to peak B (eV)							
			A	B	C	C'	C''	D	D'	E
Diamond	C <i>K</i>	theor.	-	0	4.4			12.0		34.8
		exp.	-	0	5.5			12.9		34.1
Graphite	C <i>K</i>	theor.	-4.9	0	2.5	6.6	10.3	19.4		36.0
		exp.	-6.8	0	4.4	11.2	14.7	22.1		35.1
<i>c</i> -BN	B <i>K</i>	theor.	-	0	5.5			14.2		33.2
		exp.	-	0	7.0			17.2		34.6
	N <i>K</i>	theor.	-	0	6.1			15.2		30.5
		exp.	-	0	6.4			15.5		29.8
<i>h</i> -BN	B <i>K</i>	theor.	-8.4	0	5.7			12.5	19.8	-
		exp.	-6.8	0	5.6			16.1		-
	N <i>K</i>	theor.	-6.8	0	4.1	8.2		20.9		34.3
		exp.	-6.1	0	7.2			17.6		31.8

eV. It is noted for the cubic phases that in contrast to the generally good agreement, peak D of the B *K* edge of *c*-BN (Fig. 1) is shifted by 3 eV to lower energies in the calculated spectrum. Lowering of the symmetry due to disturbed stacking order between neighboring basal planes might explain the absence of the calculated doublet peaks D/D' (B *K* of *h*-BN) in Fig. 1 and C/C' (N *K* of *h*-BN) in Fig. 3 in the actual experimental spectra. Garvie, Craven, and Brydson³¹ found a similar peak splitting in their MS calculations of the B *K* edge of *h*-BN. In the case of graphite a detailed comparison of the relative peak positions between theory and experiment (cf. Fig. 2 and Table II) reveals some substantial deviations, especially for the peaks C, C' and C''. Brydson, Brown, and Bruley²⁸ have proposed that the neglect of the energy dependence of the exchange potential⁵⁴ can result in a mismatch between the theoretical and the experimental energy scale.

The comparative study demonstrates both the potential and the limitations of the MS approach in modeling the ELNES of *K* edges of B-C-N materials. The multiple-scattering one-electron theory can be used to predict the general trends for the ELNES of B *K*, C *K*, and N *K*. Relative peak positions derived from calculations should be interpreted with great care. It has been pointed out that an impor-

tant limitation of the MS approach calculation is the mean-field neglecting effects of quasiparticle excitations^{54,55} or contributions from dipole-forbidden transitions in the experimental spectra (see, e.g. Ref. 56).

B. Predicted phases

Based on the systematic study described above the multiple-scattering approach is used further to predict the near-edge fine structure for the hypothetical phases BC₂N, BC₃, and β -C₃N₄. Those results can serve as preliminary reference spectra for materials characterization until reliable ELNES spectra are available. Furthermore, the following calculations offer the possibility to monitor from the theoretical point of view the effects of subsequent substitution of single boron atoms (as is BC₃) or BN units (as in BC₂N) into the graphitic network on the ELNES.

1. BC₂N

For simplicity, the BC₂N phase is modeled by the semi-conducting model II for a BC₂N monolayer [Fig. 4(a)] proposed by Liu, Wentzcovitch, and Cohen.¹ Since no unambiguous predictions or experimental determination of the

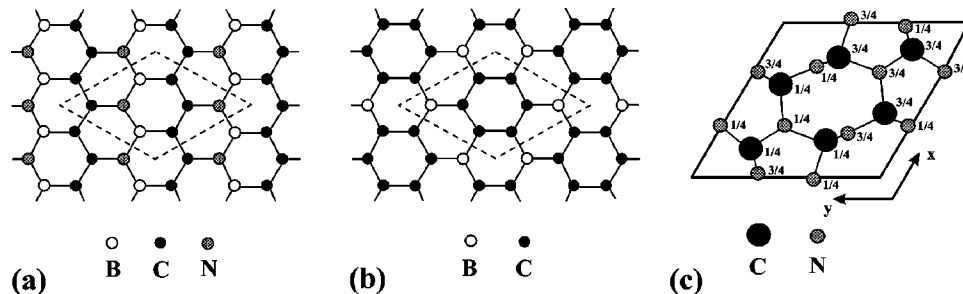


FIG. 4. Crystal structures of BC₂N (a), BC₃ (b), and β -C₃N₄ (c). The lattice parameters of BC₂N and BC₃ are $a=2.48$ Å and $c=6.68$ Å. The unit cells are enclosed by dashed lines. The crystal structure of β -C₃N₄ is projected onto the basal plane. Numbers beside the atoms are the respective values of z . The lattice parameters for β -C₃N₄ are $a=6.43$ Å and $c=2.46$ Å.

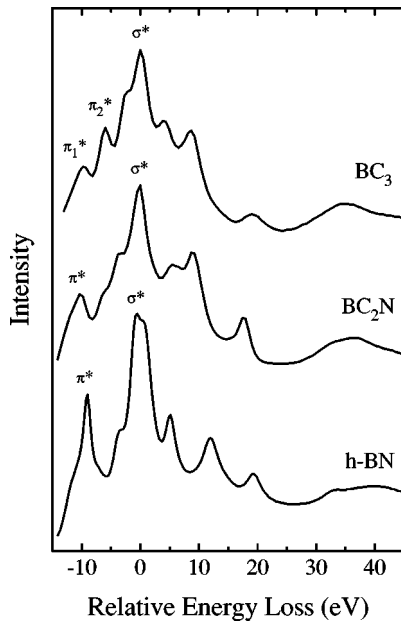


FIG. 5. Theoretical B K ELNES of BC_2N and BC_3 in comparison to h -BN. The σ^* peaks are shifted to 0 eV.

stacking sequences for BC_2N are available to date, we have decided to use the graphitelike AB stacking.

The calculated near-edge structures of the K edges are displayed in Figs. 5–7. The B K , C K , and N K features show consistently graphitelike appearance. All three spectra exhibit a sharp π^* peak, a broader σ^* peak, a feature between 25 and 35 eV, and a broad EXELFS peak. The separations of the calculated π^* and σ^* features of BC_2N are summarized in Table III in comparison to some experimental EELS results in the literature.^{4,9,57} The relative peak separation values of the theoretical K edges match the measured data within an error of 0.5 eV. However, structurally well-characterized BC_2N reference samples are not available to

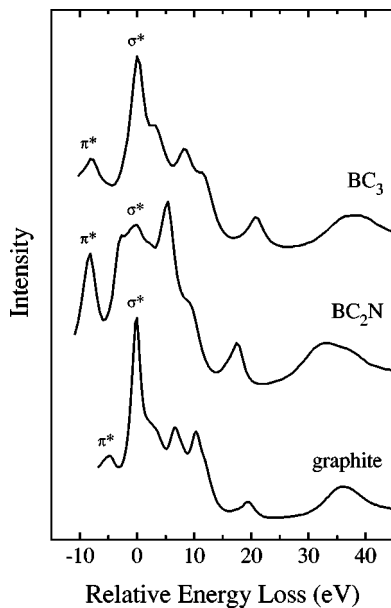


FIG. 6. Theoretical C K ELNES of BC_2N and BC_3 in comparison to graphite. The σ^* peaks are shifted to 0 eV.

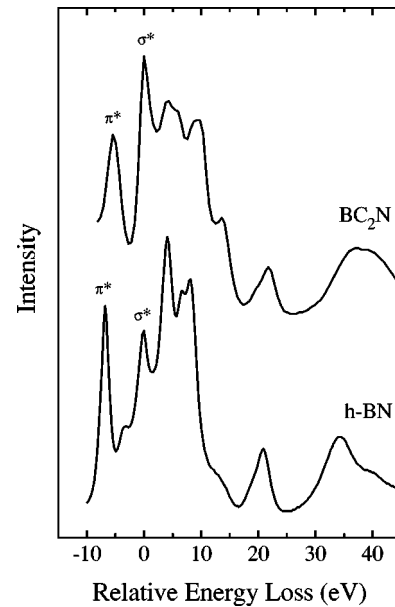


FIG. 7. Theoretical N K ELNES of BC_2N in comparison to h -BN. The σ^* peaks are shifted to 0 eV.

the knowledge of the authors. The separation values given in Table III are from boron-carbon-nitrogen hybrid phases with stoichiometries close to BC_2N .

Comparison with the experimental K edges of h -BN makes evident that both the B K and the N K edges do not have characteristic dissimilarities which would allow an unambiguous identification of BC_2N . It is only the marked changes in the σ^* transition region of the C K edge for BC_2N which might serve as a fingerprint for this phase.

2. BC_3

Figure 4(b) shows the atomic arrangement in the basal plane of BC_3 originally suggested in Ref. 5. The graphitelike AB stacking which most likely is the stable phase² is used to build up the cluster for the MS calculation. The spectra for the two inequivalent atom positions have been calculated separately and weighted to equal amounts in the presented spectra.

The calculated ELNES of the B K edge (Fig. 5) exhibits a doublet of sharp π^* peaks separated by 3.5 eV. The prediction of these two peaks agrees with previous density-of-states (DOS) calculations,^{2,3} where the separation is approximately 3.0 eV. This splitting of the π band is attributed to the lowering in translational symmetry caused by the ordered

TABLE III. Values of the separation between the π^* and σ^* features (± 0.5 eV) for the corresponding K edges of BC_2N .

	$\pi^* - \sigma^*$ Separation (eV)		
	B K	C K	N K
MS Calculations	8.5	7.5	5.5
Kouvetakis (Ref. 4)	7.0	6.5	6.0
Weng-Sieh (Ref. 9)	8.0	7.0	6.0
Sasaki (Ref. 57)	6.0	7.5	5.5

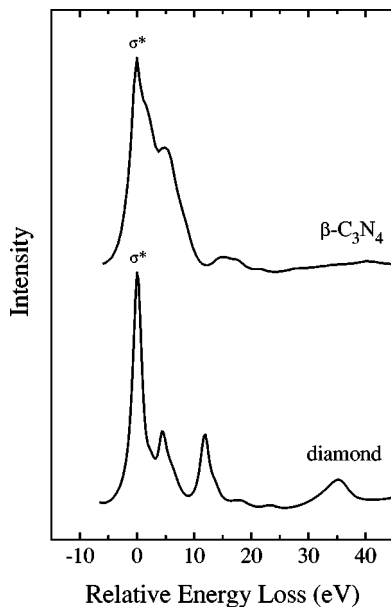


FIG. 8. Theoretical C K ELNES of β - C_3N_4 in comparison to diamond. The σ^* peaks are shifted to 0 eV.

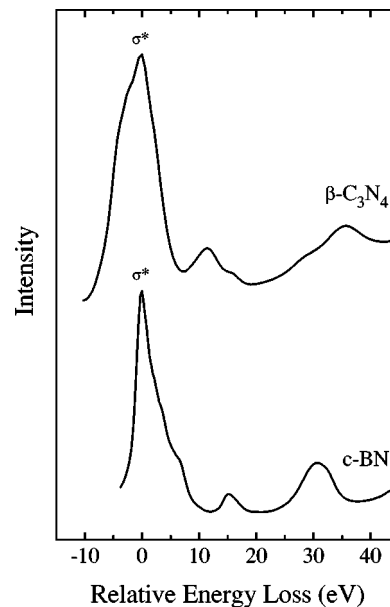


FIG. 9. Theoretical N K ELNES of β - C_3N_4 in comparison to c -BN. The σ^* peaks are shifted to 0 eV.

presence of boron in the graphitic structure.³ In reference to the mentioned DOS calculations two π^* features in the C K ELNES are expected, but this is not borne out by the MS calculation. Only a single π^* feature is present making the spectrum look very similar to graphite. There is also some experimental evidence in the electron energy-loss spectra from a thin sample of BC_3 .⁵⁸ They show two distinct π^* peaks for B K separated by 2.6 eV but only one for C K which might be related to the limited energy resolution of this experimental ELNES. Expect for the double π^* peak there are no distinct differences between the B K of BC_3 and BC_2N .

3. β - C_3N_4

Finally the K edges of the hypothetical carbon nitride solid β - C_3N_4 were calculated. The model in Fig. 4(c) displays the crystal structure of β - C_3N_4 projected onto the basal plane. The unit cell is hexagonal and contains two formula units (14 atoms). Each sp^3 -hybridized carbon atom is tetrahedrally surrounded by nitrogen atoms, whereas the sp^2 -hybridized nitrogen atoms are in a nearly trigonal planar geometry. This three-dimensional covalent network is a good prototype for the study of cubic C_3N_4 even though the bonding is not exclusively sp^3 .^{11,16} Thus it is expected that the ELNES of the C K and N K edges are similar to that of diamond and c -BN.

The calculated K ELNES of β - C_3N_4 (Figs. 8 and 9) clearly illustrate the cubic character for this phase exhibiting no π^* feature. A distinct difference to diamond is found in the C K ELNES of β - C_3N_4 only for the higher energy features above the dominant σ^* peak. These peaks are strongly attenuated for the C K ELNES whereas the N K ELNES is nearly the same than for c -BN. One possible explanation is the incomplete tetrahedral coordination resulting in a strong attenuation of the features for C K at higher energies.

V. CONCLUSION

We have presented one-electron multiple-scattering calculations of the K edges of various phases in the ternary boron-carbon-nitrogen phase diagram. For cubic diamond, graphite, c -BN, and h -BN multiple-scattering calculations are able to reproduce the main features and the relative intensity trends of the experimental data. Differences in the peak positions are mainly attributed to quasiparticle effects.^{54,55}

This systematic investigation lays the groundwork for the near-edge structure calculations of a great variety of novel phases expected in the B-C-N system. Multiple-scattering calculations have been used to predict the the K ELNES for BC_2N , BC_3 , and β - C_3N_4 . The spectra for BC_2N and BC_3 reveal mainly graphitic features, whereas the latter has near-edge features similar to those of diamond and c -BN. However, distinct features in the ELNES have been discussed which may allow the identification of these phases even in small particles or multiphase materials. Notably, the B K ELNES of BC_3 exhibits two π^* features at the onset of the main σ^* peak as a consequence of the lowering in the translational symmetry caused by the substitution of boron for carbon.³ We believe that the calculations of reference spectra for BC_2N , BC_3 , and β - C_3N_4 and also for other predicted novel materials may serve as an invaluable tool for future characterization and phase determination.

ACKNOWLEDGMENTS

One of us (Ph.K.-R.) was supported by the DFG under Contract No. RU 342/11-1 and is grateful to Professor M. Rühle for helpful suggestions. The authors would like to thank Dr. R. Brydson for continuous advice for this work and the introduction to the ICXANES code.

- ¹A. Y. Liu, R. M. Wentzcovitch, and M. L. Cohen, *Phys. Rev. B* **39**, 1760 (1989).
- ²D. Tomanek, R. M. Wentzcovitch, S. G. Louie, and M. L. Cohen, *Phys. Rev. B* **37**, 3134 (1988).
- ³R. M. Wentzcovitch, M. L. Cohen, and S. G. Louie, *Phys. Lett. A* **131**, 457 (1988).
- ⁴J. Kouvetakis, T. Sasaki, C. Shen, R. Hagiwara, M. Lerner, K. M. Krishnan, and N. Bartlett, *Synth. Met.* **34**, 1 (1990).
- ⁵J. Kouvetakis, R. B. Kaner, M. L. Sattler, and N. Bartlett, *J. Chem. Soc. Chem. Commun.* **1986**, 1758.
- ⁶S. Iijima, *Nature (London)* **354**, 56 (1991).
- ⁷Y. Miyamoto, A. Rubio, M. L. Cohen, and S. G. Louie, *Phys. Rev. B* **50**, 4976 (1994).
- ⁸O. Stephan, P. M. Ajayan, C. Colliex, Ph. Redlich, J. M. Lambert, P. Bernier, and P. Lefin, *Science* **266**, 1683 (1994).
- ⁹Z. Weng-Sieh, K. Cherrey, N. G. Chopra, Y. Miyamoto, A. Rubio, M. L. Cohen, S. G. Louie, A. Zettl, and R. Gronsky, *Phys. Rev. B* **51**, 11 229 (1995).
- ¹⁰Y. Miyamoto, A. Rubio, S. G. Louie, and M. L. Cohen, *Phys. Rev. B* **50**, 18 360 (1994).
- ¹¹A. Y. Liu and M. L. Cohen, *Science* **245**, 841 (1989).
- ¹²C. Niu, Y. Z. Lu, and C. M. Lieber, *Science* **261**, 334 (1993).
- ¹³C. M. Lieber and Z. J. Zhang, *Adv. Mater.* **6**, 497 (1994).
- ¹⁴Z. Ren, Y. Du, Z. Ying, Y. Qui, X. Xiong, J. Wu, and F. Li, *Appl. Phys. Lett.* **65**, 1361 (1994).
- ¹⁵K. M. Yu, M. L. Cohen, E. E. Haller, W. L. Hansen, A. Y. Liu, and I. C. Wu, *Phys. Rev. B* **49**, 5034 (1994).
- ¹⁶A. Y. Liu and M. L. Cohen, *Phys. Rev. B* **41**, 10 727 (1990).
- ¹⁷M. Kawaguchi, *Adv. Mater.* **9**, 615 (1997).
- ¹⁸R. F. Egerton, *Electron Energy-Loss Spectroscopy in the Electron Microscope*, 2nd ed. (Plenum, New York, 1996).
- ¹⁹Ph. Redlich, J. Loeffler, P. M. Ajayan, J. Bill, F. Aldinger, and M. Rühle, *Chem. Phys. Lett.* **260**, 465 (1996).
- ²⁰R. Brydson, H. Sauer, and W. Engel, in *Transmission Electron Energy Loss Spectrometry in Material Science*, edited by M. M. Disko, C. C. Ahn, and B. Fultz (The Minerals, Metals & Materials Society, Warrendale, PA, 1992).
- ²¹Ph. Redlich, F. Banhart, Y. Lyutovich, and P. M. Ajayan, *Carbon* **36**, 561 (1998).
- ²²H. K. Schmid, *Microsc. Microanal. Microstruct.* **6**, 99 (1995).
- ²³P. E. Batson, *Phys. Rev. B* **48**, 2608 (1993).
- ²⁴P. J. Durham, J. B. Pendry, and C. H. Hodges, *Comput. Phys. Commun.* **25**, 193 (1982).
- ²⁵D. D. Vvedensky, D. K. Saldin, and J. B. Pendry, *Comput. Phys. Commun.* **40**, 421 (1986).
- ²⁶M. Kitamura, C. Sugiura, and S. Muramatsu, *Solid State Commun.* **62**, 663 (1987).
- ²⁷X. Weng, P. Rez, and H. Ma, *Phys. Rev. B* **40**, 4175 (1989).
- ²⁸R. Brydson, L. M. Brown, and J. Bruley, *J. Microsc.* **189**, 137 (1998).
- ²⁹G. Hug (unpublished).
- ³⁰D. G. McCulloch and R. Brydson, *J. Phys.: Condens. Matter* **8**, 3835 (1996).
- ³¹L. A. J. Garvie, A. J. Craven, and R. Brydson, *Am. Mineral.* **80**, 1132 (1995).
- ³²R. Brydson, A. V. K. Westwood, S. J. Rowen, B. Rand, A. R. Merchant, and D. G. McCulloch, in *Proceedings of Eurem-11*, edited by the Committee of European Societies of Microscopy (Comm. of Eur. Soc. of Microsc., Brussels, 1998).
- ³³A. Bianconi, in *X-ray Absorption: Principles, Applications and Techniques of EXAFS, SEXAFS and XANES*, edited by D. C. Koningsberger and R. Prinz (Wiley, New York, 1988).
- ³⁴D. D. Vvedensky, in *Unoccupied Electronic States*, edited by J. C. Fuggle and J. E. Inglesfield, Springer Topics in Applied Physics Vol. 69 (Springer, Berlin, 1992).
- ³⁵J. L. Beeby, *Proc. R. Soc. London, Ser. A* **A302**, 113 (1967).
- ³⁶L. V. Azaroff and D. M. Pease, in *X-ray Spectroscopy*, edited by L. V. Azaroff (McGraw-Hill, New York, 1974).
- ³⁷R. Brydson, H. Sauer, W. Engel, J. M. Thomas, E. Zeitler, N. Kosugi, and H. Kuroda, *J. Phys.: Condens. Matter* **1**, 797 (1989).
- ³⁸L. F. Mattheiss, *Phys. Rev. A* **133**, A1399 (1964).
- ³⁹T. Loucks, *Augmented Plane Wave Method* (Benjamin, New York, 1967).
- ⁴⁰F. Herman and S. Skillman, *Atomic Structure Calculations* (Prentice Hall, Englewood Cliffs, NJ, 1965).
- ⁴¹R. Brydson, D. D. Vvedensky, W. Engel, H. Sauer, B. G. Williams, E. Zeitler, and J. M. Thomas, *J. Phys. Chem.* **92**, 962 (1988).
- ⁴²R. Brydson, J. Bruley, and J. M. Thomas, *Chem. Phys. Lett.* **149**, 343 (1988).
- ⁴³K. Schwarz, *Phys. Rev. B* **5**, 2466 (1972).
- ⁴⁴P. Kopperschmidt, master thesis, Technische Universität, Berlin, 1994.
- ⁴⁵C. J. Pickard, Ph.D. thesis, Christ's College, Cambridge, 1997.
- ⁴⁶R. W. G. Wyckoff, *Crystal Structures II* (Interscience, New York, 1964).
- ⁴⁷R. A. Rosenberg, P. J. Love, and V. Rehn, *Phys. Rev. B* **33**, 4034 (1986).
- ⁴⁸N. D. Browning, J. Yuan, and L. M. Brown, *Ultramicroscopy* **38**, 291 (1991).
- ⁴⁹R. D. Leapman, P. L. Fejes, and J. Silcox, *Phys. Rev. B* **28**, 2361 (1983).
- ⁵⁰J. Loeffler, Ph.D. thesis, Max-Planck-Institut für Metallforschung, Stuttgart, 1995.
- ⁵¹M. Wibbelt, Ph.D. thesis, Westfälische Wilhelms-Universität Münster, 1999.
- ⁵²R. Brydson, *EMSA Bull.* **21**, 57 (1991).
- ⁵³M. Jaouen, G. Hug, V. Gonnet, G. Demazeau, and G. Tourillon, *Microsc. Microanal. Microstruct.* **6**, 127 (1995).
- ⁵⁴I. Davoli, A. Marcelli, A. Bianconi, M. Tomellini, and M. Fanfoni, *Phys. Rev. B* **33**, 2979 (1986).
- ⁵⁵P. J. Weijss, M. T. Czyzyk, J. F. van Acker, W. Speier, J. B. Goedkoop, H. van Leuken, H. J. M. Hendrix, R. A. de Groot, G. van der Laan, K. H. J. Buschow, G. Wiech, and J. C. Fuggle, *Phys. Rev. B* **41**, 11 899 (1990).
- ⁵⁶P. Aebi, M. Erbudak, F. Vanini, D. D. Vvedensky, and G. Kosterz, *Phys. Rev. B* **42**, 5369 (1990).
- ⁵⁷T. Sasaki and N. Bartlett (unpublished data in Ref. 1).
- ⁵⁸K. M. Krishnan, *Appl. Phys. Lett.* **58**, 1857 (1991).